JCI insight

RESEARCH ARTICLE

Fetal and amniotic fluid iron homeostasis in healthy and complicated murine, macaque, and human pregnancy

Allison L. Fisher,[1,2] Veena Sangkhae,[2] Pietro Presicce,[3] Claire A. Chougnet,[4,5] Alan H. Jobe,[5,6] Suhas G. Kallapur,[3] Sammy Tabbah,[7] Catalin S. Buhimschi,[8] Irina A. Buhimschi,[8] Tomas Ganz,[2] and Elizabeta Nemeth[2]

[1]Molecular, Cellular and Integrative Physiology Graduate Program, Graduate Programs in Bioscience, [2]Center for Iron Disorders, and [3]Neonatal-Perinatal Medicine, Department of Pediatrics, Department of Medicine, David Geffen School of Medicine, UCLA, Los Angeles, California, USA. [4]Division of Immunobiology, Cincinnati Children's Hospital Research Foundation. [5]University of Cincinnati College of Medicine, Cincinnati, Ohio, USA. [6]Division of Neonatology/Pulmonary Biology, Cincinnati Children's Hospital Research Foundation, Cincinnati, Ohio, USA. [7]Cincinnati Fetal Center, Cincinnati Children's Hospital Medical Center and Department of Obstetrics and Gynecology, University of Cincinnati College of Medicine, Cincinnati, Ohio, USA. [8]Department of Obstetrics and Gynecology, University of Illinois at Chicago College of Medicine, Chicago, Illinois, USA.

Adequate iron supply during pregnancy is essential for fetal development. However, how fetal or amniotic fluid iron levels are regulated during healthy pregnancy, or pregnancies complicated by intraamniotic infection or inflammation (IAI), is unknown. We evaluated amniotic fluid and fetal iron homeostasis in normal and complicated murine, macaque, and human pregnancy. In mice, fetal iron endowment was affected by maternal iron status, but amniotic fluid iron concentrations changed little during maternal iron deficiency or excess. In murine and macaque models of inflamed pregnancy, the fetus responded to maternal systemic inflammation or IAI by rapidly upregulating hepcidin and lowering iron in fetal blood, without altering amniotic fluid iron. In humans, elevated cord blood hepcidin with accompanying hypoferremia was observed in pregnancies with antenatal exposure to IAI compared with those that were nonexposed. Hepcidin was also elevated in human amniotic fluid from pregnancies with IAI compared with those without IAI, but amniotic fluid iron levels did not differ between the groups. Our studies in mice, macaques, and humans demonstrate that amniotic fluid iron is largely unregulated but that the rapid induction of fetal hepcidin by inflammation and consequent fetal hypoferremia are conserved mechanisms that may be important in fetal host defense.

Introduction

In healthy humans and animals, iron in plasma is bound to the carrier protein transferrin (TF). When iron supply to plasma increases, such as in iron overload disorders or with iron supplementation, or when iron utilization decreases, such as with erythropoietic suppression, TF may become saturated, causing "free" or non–TF-bound iron (NTBI) to appear in circulation (1). In humans, NTBI is detectable in amniotic fluid and fetal serum during the first trimester (2) and the beginning of the second trimester (3), when TF levels are low, but is expected to decrease with gestational age (4), as TF concentration increases in amniotic fluid (5, 6) Unlike iron-TF, NTBI is highly reactive, has the potential to catalyze the generation of reactive oxygen species in both the extracellular fluid and tissues in which it is taken up (7), and promotes the rapid growth of Gram-negative bacteria (8).

Since humans and animals cannot excrete excess iron, mechanisms have evolved to prevent iron accumulation and minimize the potential for oxidative damage or spread of certain infections. Hepcidin, a peptide hormone produced in the liver, regulates plasma iron levels and tissue iron distribution (9) by occluding ferroportin, the hepcidin receptor and only known iron exporter, and causing its degradation. In turn, this results in iron sequestration in target cells and decreased iron transport into plasma (10, 11). Hepcidin is feedback regulated by iron concentrations and erythropoietic activity and potently induced by inflammation (12–16).

Conflict of interest: TG and EN are shareholders of and scientific advisors for Intrinsic LifeSciences and Silarus Therapeutics and consultants for Ionis Pharmaceuticals, Protagonist, and Vifor. TG is a consultant for Akebia.

Submitted: November 27, 2019
Accepted: January 22, 2020
Published: February 27, 2020.

Reference information: *JCI Insight*. 2020;5(4):e135321. https://doi.org/10.1172/jci.insight.135321.

During pregnancy, iron is critical for the development of the fetus and placenta and for maternal erythropoietic expansion (17, 18). To accommodate these changes, maternal hepcidin is suppressed to nearly undetectable levels in the second and third trimesters (19–22); this is thought to facilitate increased dietary iron absorption, release of iron from stores, and iron transfer to the fetus (23). Thus, inappropriately elevated maternal hepcidin, as would be expected during inflammation, could be detrimental by compromising iron availability for placental uptake and transfer to the fetus.

In addition to maternal hepcidin, fetal hepcidin could also determine placental iron transfer during pregnancy because ferroportin is localized on the basal side of placental syncytiotrophoblast, facing fetal circulation (24, 25). Indeed, a transgenic mouse model of hepcidin overexpression confirmed that fetal hepcidin is capable of regulating placental ferroportin, causing severe fetal iron deficiency and decreased viability (26, 27). Under normal physiological conditions, endogenous fetal hepcidin expression is low (26, 27) and does not affect iron transfer across the placenta (22). However, certain clinical conditions, such as intraamniotic infection or inflammation (IAI), can induce fetal hepcidin (28). Whether hepcidin regulates iron homeostasis in amniotic fluid and fetal blood has not been explored.

Here, we evaluated amniotic fluid and fetal iron homeostasis in normal and complicated murine, rhesus macaque, and human pregnancy. We found that amniotic fluid iron was not strongly regulated by fetal hepcidin or by maternal iron status but that fetal plasma iron during inflammation or infection was regulated by fetal hepcidin, which may be an important protective mechanism for fetal host defense.

Results

Effect of maternal iron status on fetal and amniotic fluid iron homeostasis in mice. To evaluate amniotic fluid iron homeostasis during normal pregnancy, we compared amniotic fluid iron levels during normal mouse gestation from E12.5 to E18.5. Iron concentrations in amniotic fluid were similar between E12.5 and E16.5 and increased sharply before term at E18.5 ($P < 0.001$) (Figure 1A). We next determined how changes in maternal iron status alter iron concentrations in fetal serum and amniotic fluid by comparing E18.5 iron-replete pregnancies (those with normal iron stores) to iron-deficient (diet-induced) and iron-loaded (hepcidin knockout) pregnancies. We confirmed changes in maternal iron status by showing that serum iron concentrations were lower in iron-deficient dams and higher in iron-loaded dams compared with iron-replete controls and that liver iron concentrations were increased in iron-loaded dams (Table 1). Hemoglobin, hematocrit, mean corpuscular volume, and mean corpuscular hemoglobin were all lower in iron-deficient dams and higher in iron-loaded dams compared with iron-replete controls (Table 1).

In fetal serum, iron concentrations were lower with maternal iron deficiency and higher with maternal iron overload compared with those from iron-replete mothers (Figure 1B) (both $P < 0.001$). Compared with fetal serum, iron concentrations in amniotic fluid were relatively spared from changes in maternal iron status (Figure 1C). In all dams, fetal serum iron correlated with maternal serum iron concentrations ($r = 0.846$, $P < 0.001$) (Figure 1D), but amniotic fluid iron concentrations showed only weak nonsignificant correlation with maternal serum iron ($r = 0.465$, $P = 0.110$) (Figure 1E). Fetal serum iron strongly correlated with amniotic fluid iron ($r = 0.657$, $P < 0.001$) (Figure 1F).

To assess whether the fetus or amniotic fluid could be vulnerable to infection because of NTBI, we evaluated whether maternal iron status alters TF concentrations and TF saturations (TSATs) in the fetus and amniotic fluid. Comparing the 3 compartments in iron-replete mouse pregnancy — maternal serum, fetal serum, and amniotic fluid — we found the highest TF concentrations in maternal serum and lowest in amniotic fluid ($P < 0.001$) (Figure 2A). As a result, fetal serum and amniotic fluid had much higher TSAT (60%–70%) than maternal serum (Figure 2B) ($P = 0.007$).

Considering the effect of maternal iron status on maternal iron parameters, TF concentrations were similar between iron-deficient, iron-replete, and iron-loaded dams (Figure 2C). As expected, maternal serum TSAT was lower with iron deficiency ($P = 0.023$) and higher with iron overload ($P < 0.001$) (Figure 2D), reflecting changes in serum iron (Table 1).

In fetal serum (Figure 2, E and F), TSAT was lower in iron-deficient pregnancy ($P < 0.001$) due to low serum iron concentrations (Figure 1B). TSATs were similar between iron-loaded and iron-replete groups, despite the difference in fetal serum iron (Figure 1B), because of increased fetal TF levels in iron-loaded pregnancy ($P < 0.001$).

In amniotic fluid, TF levels were slightly lower in iron-deficient and iron-loaded pregnancy compared with

Table 1. E18.5 maternal iron and hematological parameters in murine pregnancy

	Iron deficient	*P* value	Iron replete	*P* value	Iron loaded
	E18.5 (*n* = 4)	Iron deficient vs. replete	E18.5 (*n* = 5)	Iron replete vs. loaded	E18.5 (*n* = 5)
Serum iron (μM)	5.84 ± 0.78	*P* = 0.002	21.59 ± 9.73	*P* < 0.001	48.67 ± 1.71
Liver (μg/g)	7.83 ± 0.13	*P* = 0.991	8.59 ± 2.95	*P* < 0.001	476.0 ± 171.95
RBC (10^6/μL)	7.57 ± 0.19	*P* = 0.064	7.66 ± 0.12	*P* = 0.064	7.80 ± 0.08
Hb (g/dL)	9.40 ± 0.35	*P* = 0.009	10.22 ± 0.52	*P* < 0.001	12.20 ± 0.25
HCT (%)	36.25 ± 1.00	*P* < 0.001	40.40 ± 1.58	*P* < 0.001	45.48 ± 0.95
MCV (fL)	47.90 ± 0.74	*P* < 0.001	52.70 ± 1.78	*P* < 0.001	58.28 ± 1.03
MCH (pg)	12.40 ± 0.36	*P* = 0.011	13.32 ± 0.58	*P* < 0.001	15.64 ± 0.34

Iron and hematological parameters of E18.5 pregnant iron-deficient WT dams (fed low-iron diet), iron-replete WT dams (fed standard diet), and iron-loaded hepcidin knockout dams (fed standard diet). Data are presented as mean ± SD. Hb, hemoglobin; HCT, hematocrit; MCV, mean corpuscular volume; MCH, mean corpuscular hemoglobin. Statistical differences between groups were determined by 1-way ANOVA followed by Holm-Sidak method for multiple comparisons.

iron-replete pregnancy (both $P = 0.02$) (Figure 2G), but TSAT was relatively high in all the groups, particularly in the iron-loaded group ($P = 0.012$) (Figure 2H).

Our data demonstrate that, in mouse pregnancy, amniotic fluid iron concentrations are less affected by maternal iron status than fetal serum iron. Although amniotic fluid iron concentrations are relatively low, TSAT of the fluid is high, a condition known to be associated with the presence of NTBI. Fetal serum also had high TSAT under iron-replete conditions, increasing the risk of NTBI generation.

Effect of maternal systemic inflammation on fetal iron homeostasis in mice. Fetal hepcidin expression can be induced by IAI (28), but whether fetal hepcidin can regulate iron homeostasis in the amniotic fluid or fetal circulation is unknown. We evaluated the contribution of fetal hepcidin to the fetal and amniotic iron homeostasis in the presence of maternal inflammation. We induced systemic maternal inflammation in mice by injecting pregnant, iron-replete WT dams with a single subcutaneous dose of LPS on E15.5 (~80% gestation) for 6 or 24 hours. As expected, LPS treatment induced mRNA expression of inflammatory marker serum amyloid A-1 (*Saa-1*) in maternal liver ($P < 0.001$) (Figure 3A). Furthermore, LPS treatment transiently induced maternal hepatic hepcidin (*Hamp*) mRNA and maternal hepcidin protein in serum (both $P = 0.001$) and caused maternal hypoferremia ($P < 0.001$) (Figure 3, B–D). In response to maternal LPS treatment, fetal hepatic hepcidin expression transiently increased within 6 hours and returned to normal levels within 24 hours ($P < 0.001$) (Figure 3E). Following induction of hepcidin synthesis by the fetal liver, both fetal serum hepcidin ($P < 0.001$) and amniotic fluid hepcidin ($P = 0.008$) were elevated 24 hours after maternal LPS injection (Figure 3, F and G). Amniotic fluid hepcidin strongly correlated with fetal serum hepcidin ($r = 0.913$, $P = 0.002$) (Supplemental Figure 1; supplemental material available online with this article; https://doi.org/10.1172/jci.insight.135321DS1). However, hypoferremia occurred only in fetal serum ($P = 0.005$), whereas amniotic fluid iron concentrations were similar between control and LPS-injected groups (Figure 3, H and I). Therefore, fetal hepcidin is responsive to acute inflammation, causing hypoferremia in fetal circulation but not in amniotic fluid.

Fetal iron homeostasis during IAI in rhesus macaques. We evaluated the fetal response to intraamniotic rather than systemic maternal inflammation using a rhesus macaque model of IAI. On gestational day 130 (80% of the duration of pregnancy), pregnant dams received a single intraamniotic injection of LPS for 16 hours or *Ureaplasma* for 3 days. In these models with intraamniotic injections, the inflammation is largely localized to the intrauterine compartment, including the fetus (29, 30). To evaluate maternal systemic inflammation, we measured cytokines TNF-α, MCP-1, IL-1β, and IL-6 in maternal plasma (Figure 4, A–D). We did not detect increases in any cytokines with LPS injection and, with *Ureaplasma* infection, only MCP-1 was elevated ($P = 0.005$). Consistent with the lack of significant increases in cytokines, we did not detect any changes in maternal plasma hepcidin or iron with intraamniotic LPS or *Ureaplasma* (Figure 5, A and D).

In rhesus macaque cord blood plasma, following intraamniotic LPS injection, we detected increased TNF-α ($P = 0.016$), MCP-1 ($P < 0.001$), IL-1β ($P < 0.001$), and IL-6 ($P = 0.002$) (Figure 4, E–H). In amniotic fluid, LPS similarly induced TNF-α ($P = 0.003$), MCP-1 ($P = 0.002$), IL-1β ($P = 0.003$), and IL-6 ($P = 0.002$) (Figure 4, I–L), confirming that inflammation was restricted to the fetal compartment.

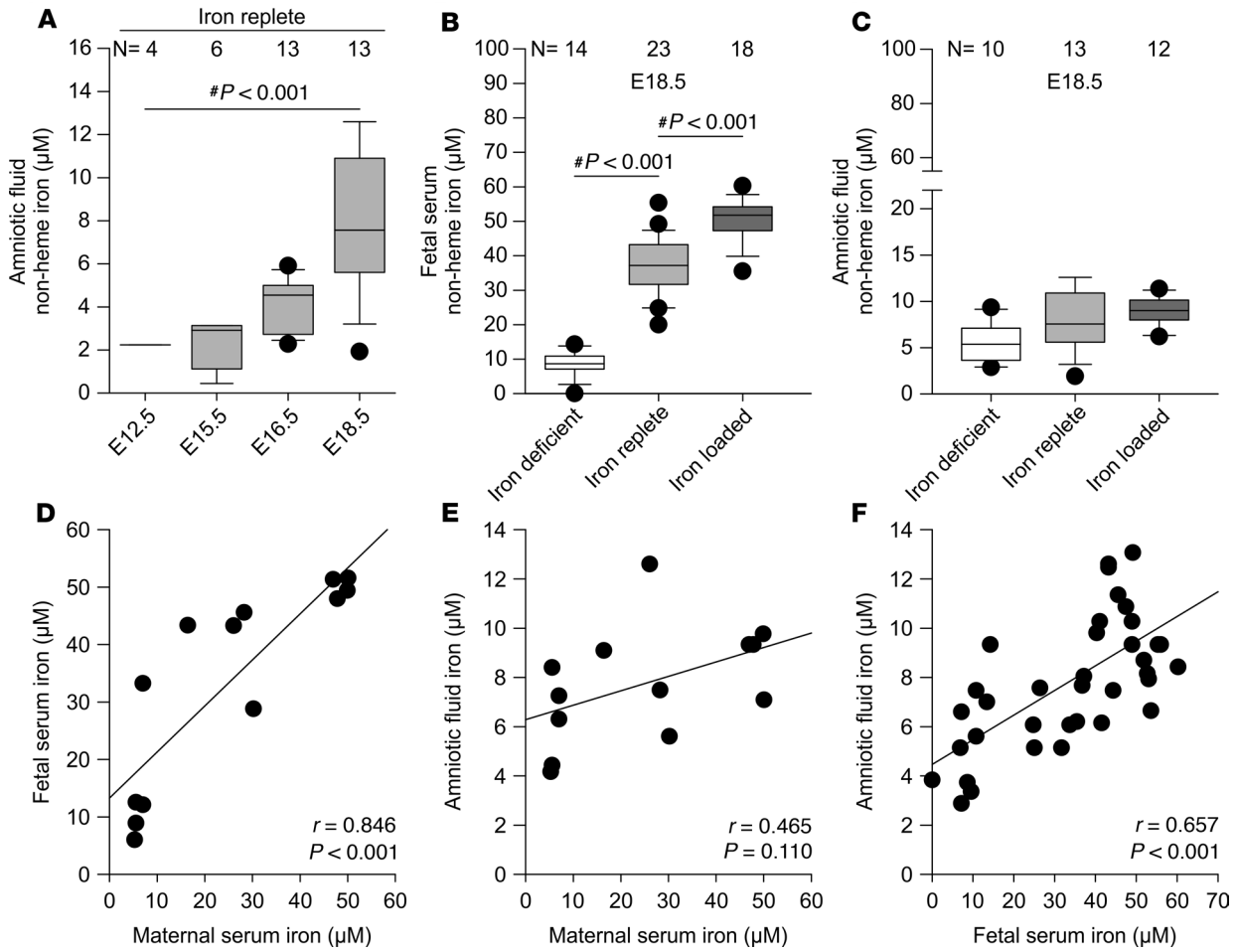

Figure 1. Effect of maternal iron status on fetal and amniotic fluid iron parameters in mice. Maternal iron deficiency was induced by feeding low-iron diet to WT dams starting on E10.5 until analysis at E18.5. Iron-loaded dams were hepcidin-deficient mice fed standard chow. Both iron-deficient and iron-loaded dams were compared with iron-replete WT dams fed standard chow. (**A**) Amniotic fluid iron concentrations from iron-replete dams from E12.5 to E18.5. (**B** and **C**) Fetal serum and amniotic fluid iron from iron-deficient, iron-replete, and iron-loaded dams on E18.5. (**D**–**F**) Pearson correlations between maternal serum iron, fetal serum iron, and amniotic fluid iron on E18.5. For **D** and **E**, maternal serum iron was correlated to the litter average for fetal serum iron or amniotic fluid iron. Statistical differences between groups were determined by 1-way ANOVA on ranks followed by Dunn's method for multiple comparisons (as indicated by #). The number of animals is indicated above the box plot for each panel.

Furthermore, LPS strongly induced fetal hepcidin in cord blood plasma and amniotic fluid (both P = 0.001) (Figure 5, B and C). Similar to that in mice, amniotic fluid hepcidin strongly correlated with cord blood hepcidin in rhesus macaques (r = 0.992, P < 0.001) (Supplemental Figure 2). Induction of fetal hepcidin by intraamniotic LPS resulted in profound hypoferremia in cord blood plasma (P < 0.001) but not amniotic fluid (Figure 5, E and F). Cord blood plasma hepcidin correlated with cord blood cytokines TNF-α (r = 0.731, P = 0.003), MCP-1 (r = 0.739, P = 0.003), IL-1β (r = 0.809, P < 0.001), and IL-6 (r = 0.808, P < 0.001) (Supplemental Figure 3, A–D). Amniotic fluid hepcidin correlated with amniotic fluid cytokines TNF-α (r = 0.910, P < 0.001), MCP-1 (r = 0.906, P < 0.001), IL-1β (r = 0.723, P = 0.003), and IL-6 (r = 0.622, P = 0.018) (Supplemental Figure 3, E–H). We did not detect any changes in iron, hepcidin, or cytokines in cord blood plasma or amniotic fluid with intraamniotic *Ureaplasma* infection.

Thus, similar to the mouse model, fetal hepcidin in rhesus macaques was induced by acute inflammation, causing hypoferremia in fetal circulation, without altering iron concentrations in amniotic fluid.

Amniotic fluid and cord blood iron homeostasis in healthy and complicated human pregnancy. We next evaluated amniotic fluid iron and hepcidin in human pregnancies associated with IAI. All samples were collected at amniocentesis before 32 weeks of gestation (Table 2). The samples were eventually analyzed in the following 4 groups: pregnancies with IAI and with preterm delivery (PosIAI/PTB, n = 72), pregnancies without IAI and with preterm delivery (NegIAI/PTB, n = 22), pregnancies without IAI and with term delivery (NegIAI/TB, n = 20), and pregnancies without IAI but with maternal systemic inflammatory response

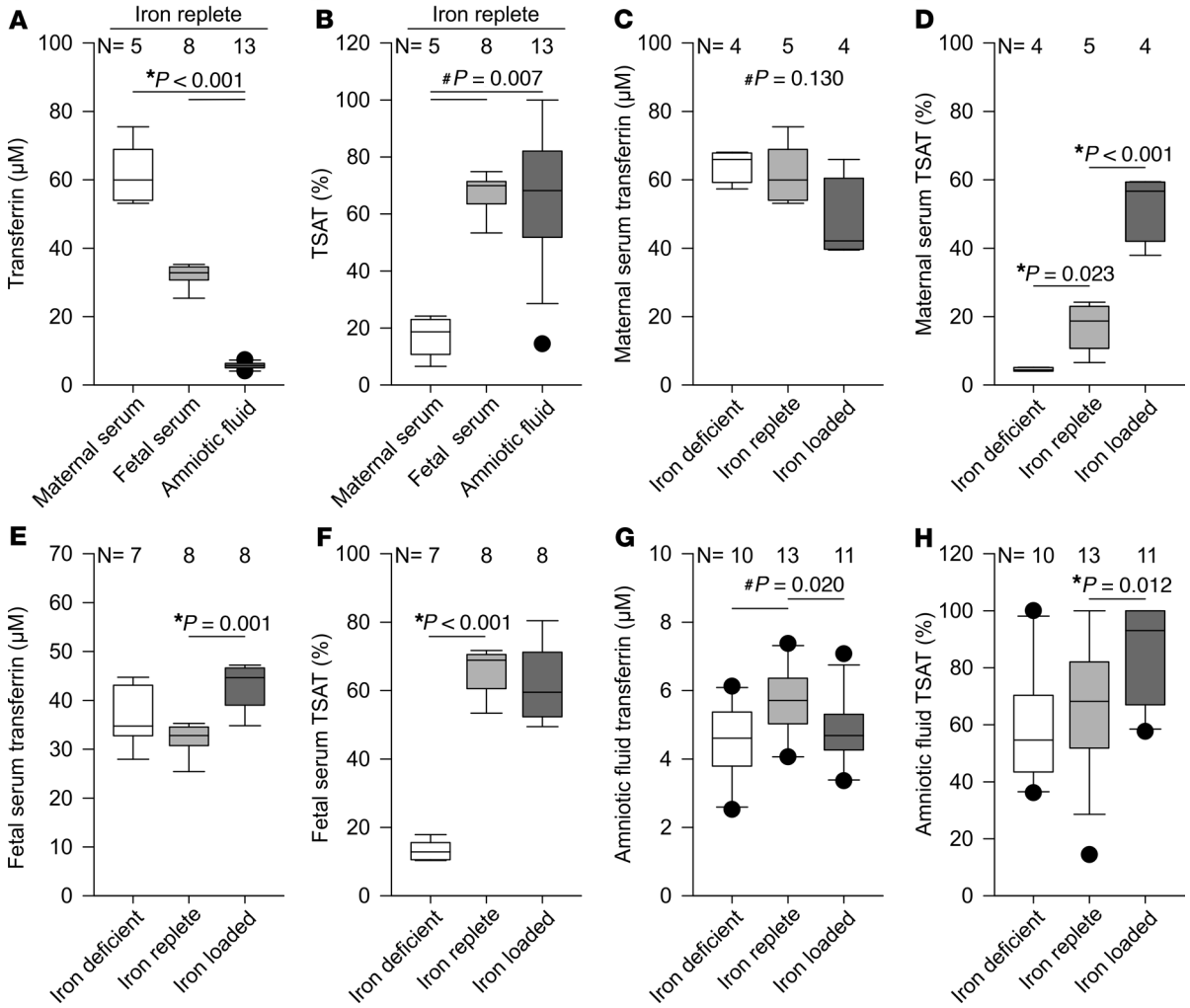

Figure 2. Effect of maternal iron status on fetal and amniotic fluid transferrin and transferrin saturation in mice. Maternal iron deficiency was induced by feeding low-iron diet to WT dams starting on E10.5 until analysis at E18.5. Iron-loaded dams were hepcidin-deficient mice fed standard chow. Both iron-deficient and iron-loaded dams were compared with iron-replete WT dams fed standard chow. (**A** and **B**) Transferrin concentrations and TSAT in maternal serum, amniotic fluid, and fetal serum on E18.5 in iron-replete pregnancy. (**C** and **D**) Maternal transferrin concentration and TSAT and (**E**–**H**) fetal serum and amniotic fluid transferrin concentration and TSAT from iron-deficient, iron-replete, and iron-loaded pregnancies on E18.5. Statistical differences between groups were determined by 1-way ANOVA for normally distributed values followed by Holm-Sidak method for multiple comparisons (as indicated by *) or 1-way ANOVA on ranks followed by Dunn's method for multiple comparisons (as indicated by #). The number of animals is reported above the box plot for each panel.

syndrome (SIRS) and term delivery (NegIAI/TB/SIRS, n = 10). Adjusting for gestational age, amniotic fluid hepcidin was significantly different between the groups (P = 0.008) and was higher in those positive for IAI and lower in those without IAI (Table 2). Amniotic fluid IL-6 was also elevated in the PosIAI/PTB group (P < 0.001) (Table 2). Despite differences in hepcidin, amniotic fluid iron concentrations were similar between all the groups (Table 2). Furthermore, TSAT remained under 20% in all the groups (Table 2).

Although iron is not regulated by inflammation or infection in human amniotic fluid, we next addressed whether the human fetus can upregulate its own hepcidin during inflammation to regulate iron homeostasis in fetal blood. To address this question we used a separate cohort, where umbilical vein cord blood plasma was sampled at delivery from singleton preterm human fetuses (<34 weeks of gestation) with or without antenatal exposure to IAI, as determined by elevated IL-6 in cord blood plasma (P < 0.001). In this cohort we confirmed that exposure to IAI resulted in elevated fetal hepcidin and IL-6 in cord blood plasma (both P < 0.001) (Figure 6, A and B). Coinciding with elevated hepcidin in circulation, exposure to IAI also resulted in lower cord blood plasma iron concentrations and lower TSAT compared with those in healthy fetuses (P < 0.001 and P = 0.002) (Figure 6, C and D). Thus, samples from human fetuses with antenatal exposure to IAI demonstrated induction of fetal hepcidin and hypoferremia, similar to responses seen in our animal models.

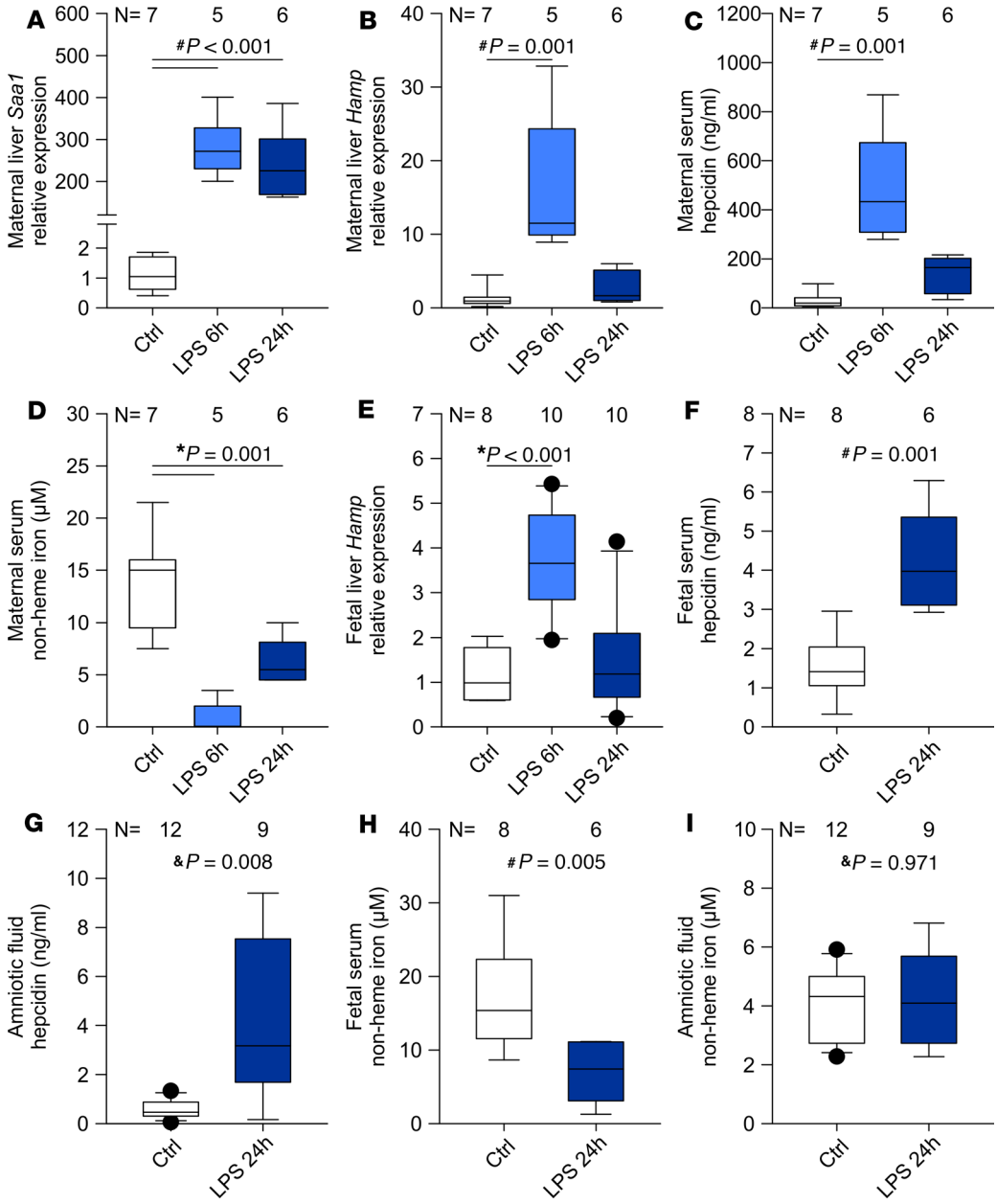

Figure 3. Effect of maternal systemic inflammation on fetal iron homeostasis in mice. To induce maternal systemic inflammation during pregnancy, iron-replete WT dams received a single subcutaneous injection of 0.5 μg/g LPS on E15.5 for 6 or 24 hours. (**A**) Maternal liver serum amyloid A-1 (*Saa1*) and (**B**) hepcidin (*Hamp*) mRNA expression normalized to *Hprt*. Measurements in maternal serum: (**C**) hepcidin and (**D**) iron. Fetal (**E**) liver hepcidin mRNA expression normalized to *Rpl4*, (**F**) serum hepcidin, and (**G**) serum iron. Amniotic fluid (**H**) hepcidin and (**I**) iron. Statistical differences between groups were determined by 1-way ANOVA for normally distributed values followed by Holm-Sidak method for multiple comparisons (as indicated by *), 2-tailed Student's *t* test for normally distributed values (as indicated by #), or Mann-Whitney *U* test (as indicated by &). The number of animals is reported above the box plot for each panel.

Discussion

During pregnancy, adequate delivery of iron is essential for normal development of the fetus and placenta. Moreover, tight control of iron concentrations may be protective against certain infections. However, whether fetal or amniotic fluid iron levels are regulated during healthy or complicated pregnancy has not been reported. In this study, we describe amniotic fluid and fetal iron homeostasis in healthy and complicated murine, rhesus macaque, and human pregnancy.

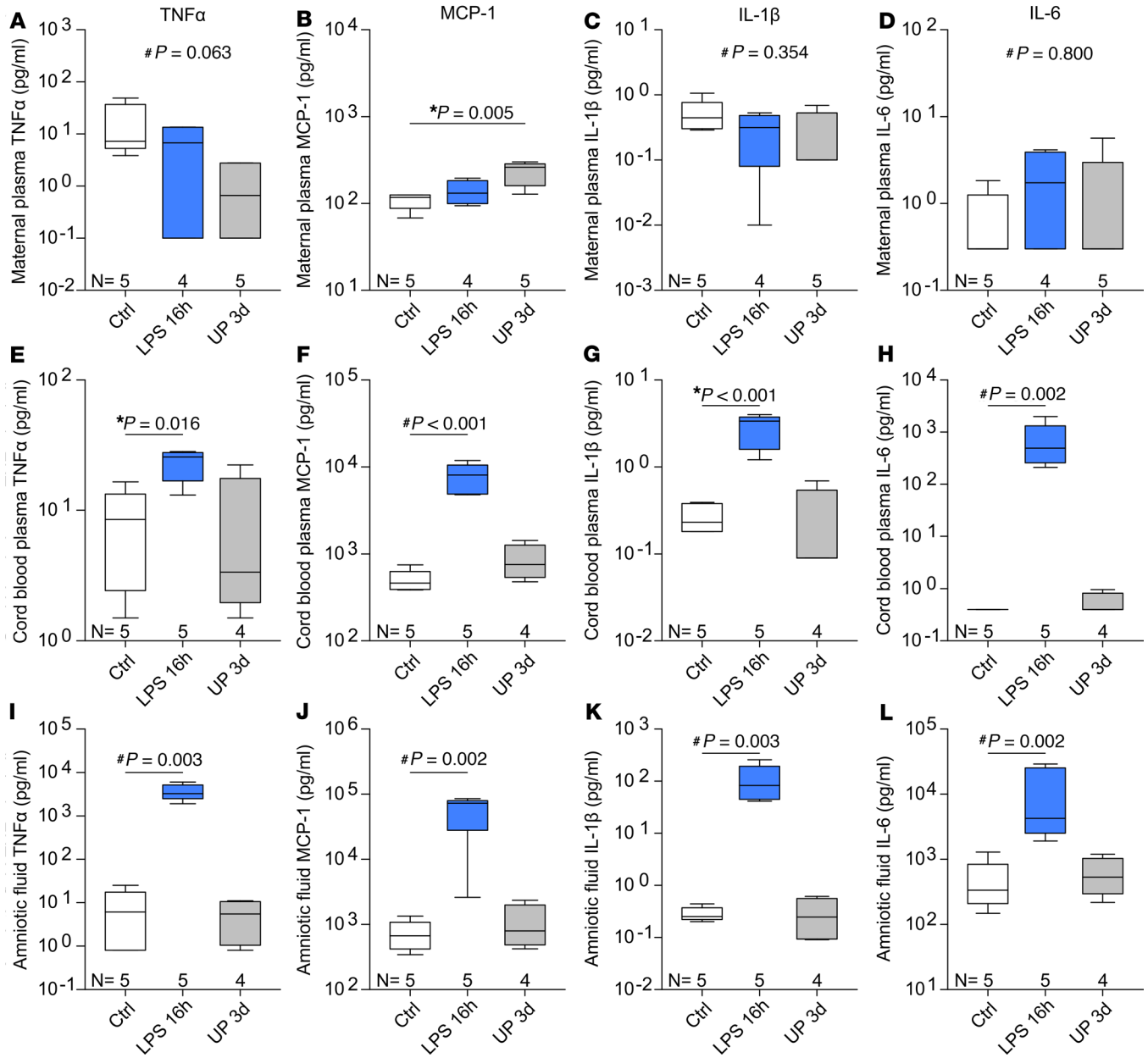

Figure 4. Cytokines in maternal plasma, cord blood plasma, and amniotic fluid during IAI in rhesus macaques. Pregnant rhesus macaques at 130 days gestation received a single intraamniotic injection of LPS (1 mg) for 16 hours or *Ureaplasma parvum* serovar 1 (1×10^7 CFU) for 3 days. Cytokines TNF-α, MCP-1, IL-1β, and IL-6 were measured in (**A**–**D**) maternal plasma, (**E**–**H**) cord blood plasma, and (**I**–**L**) amniotic fluid at delivery. Statistical differences between groups were determined by 1-way ANOVA for normally distributed values followed by Holm-Sidak method for multiple comparisons (as indicated by *) or 1-way ANOVA on ranks followed by Dunn's method for multiple comparisons (as indicated by #). A subset of these data was previously reported (30, 44). The number of animals is reported on the *x* axis of each panel.

In humans, iron concentrations in amniotic fluid were reported to be approximately 2–3 times lower than those in maternal plasma (31–33). In non-iron–supplemented pregnant women, iron concentrations in amniotic fluid do not correlate with those in maternal blood when assessed at 17 weeks of gestation (32). However, in iron-supplemented women in the second trimester, concentrations of iron in amniotic fluid were linearly correlated to concentrations in maternal blood (31), suggesting that iron in amniotic fluid can be increased through iron supplementation. Using mouse models, we evaluated whether changes in maternal iron status during pregnancy alter fetal and amniotic fluid iron homeostasis. We found that, while fetal serum iron endowment was strongly dependent on maternal iron status, amniotic fluid iron was less affected by either maternal iron deficiency or excess. Compared with maternal serum from normal mouse

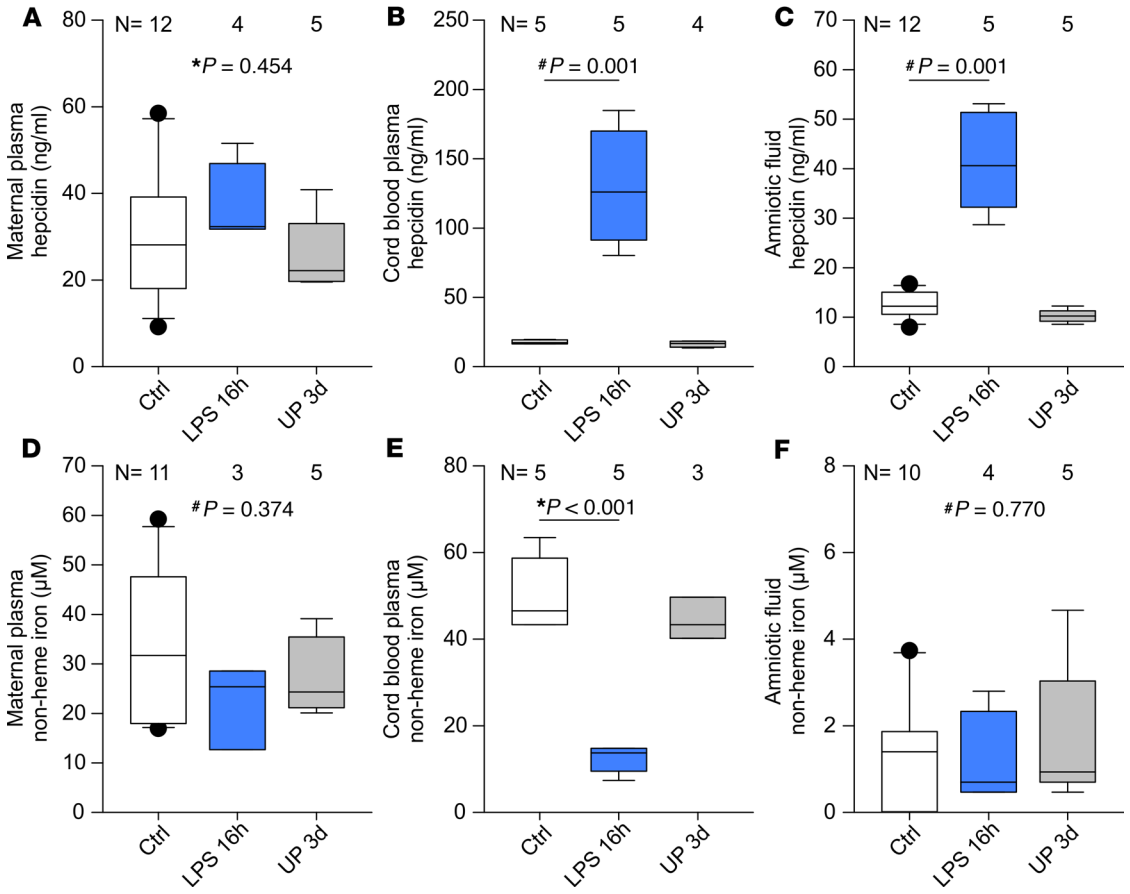

Figure 5. Iron parameters in maternal plasma, cord blood plasma, and amniotic fluid during IAI in rhesus macaques. Pregnant rhesus macaques received a single intraamniotic injection of LPS (1 mg) for 16 hours or *Ureaplasma parvum* serovar 1 (1×10^7 CFU) for 3 days. (**A**–**C**) Hepcidin and (**D**–**F**) iron measurements in maternal plasma, cord blood plasma, and amniotic fluid. The control group included samples taken before injection or after saline injection (there was no difference between the 2 groups). The saline group included only samples at delivery after saline injection. Statistical differences between groups were determined by 1-way ANOVA for normally distributed values followed by Holm-Sidak method for multiple comparisons (as indicated by *) or 1-way ANOVA on ranks followed by Dunn's method for multiple comparisons (as indicated by #). The number of animals is reported above the box plot for each panel.

pregnancy, both fetal serum and amniotic fluid had relatively high TSAT, even under iron replete conditions (~60% in fetal serum/amniotic fluid vs. <20% in maternal serum). Although maternal iron overload did not significantly increase amniotic fluid iron concentrations (which were generally low), TSAT approached 100%, suggesting that maternal iron supplementation could cause the appearance of NTBI in amniotic fluid.

Under normal conditions, iron in plasma is bound to TF with very high affinity, with TSAT ranging from 20% to 50%. Although very few bacterial species can use TF-bound iron, iron availability to microbes increases when NTBI appears in circulation in iron overload diseases or with iron supplementation. In our study, compared with murine amniotic fluid TSAT of >60%, human amniotic fluid collected between 21 and 36 weeks of gestation had TSAT under 20% and human cord blood had TSAT under 40%, suggesting that there is sufficient apoTF to bind iron and decrease the risk of NTBI appearance. Several earlier studies in human amniotic fluid report inhibition of bacterial growth of *E. coli*, *Staphylococcus aureus*, and *Bacillus subtilis* in amniotic fluid with excess apoTF concentrations (4, 34–36), suggesting an important role of the iron-binding capacity of TF to limit iron availability to bacteria.

Inflammation has a potent effect on iron homeostasis. Known as hypoferremia of inflammation, the cytokine-driven increase in hepcidin (13) decreases iron transport into plasma, so that NTBI is not available to stimulate the growth of certain pathogenic bacteria. We investigated whether the fetus shows a hypoferremic response to inflammation in utero. In our mouse model of systemic maternal inflammation, the fetuses responded by acutely increasing mRNA synthesis of hepcidin in the liver and serum hepcidin within 6–24 hours and lowering serum iron within 24 hours. LPS treatment of pregnant mice, however, also induced

Table 2. Amniotic fluid iron homeostasis in healthy and complicated human pregnancy

	PosIAI/PTB *n* = 72	NegIAI/TB/SIRS *n* = 10	NegIAI/PTB *n* = 22	NegIAI/TB *n* = 20	*P* value by factorial ANCOVA
IAI	Yes	No	No	No	
GA at amniocentesis (mean ± SD)	26.6 ± 2.9	31.5 ± 3.6	30.5 ± 2.4	29.03 ± 4.0	
GA at delivery (mean ± SD)	26.8 ± 2.9	39.3 ± 1.2	31.2 ± 2.3	38.9 ± 1.1	
AF hepcidin (ng/mL)	8.9	5.7	3.7[A]	2.0[B]	$P = 0.008$
AF IL-6 (pg/mL)	67.0	4.4[A]	5.1[C]	1.5[C]	$P < 0.001$
AF non-heme iron (μM)	2.2	2.4	2.4	2.1	$P = 0.981$
AF TSAT (%)	9.2	14.2	13.1	10.6	$P = 0.309$

Amniotic fluid was sampled at amniocentesis from women that presented with clinical indication of intraamniotic infection. Amniotic fluid was collected by ultrasound-guided amniocentesis from mothers that ultimately delivered preterm with intraamniotic infection (PosIAI/PTB) or without intraamniotic infection (NegIAI/PTB), mothers that ultimately delivered at term but with systemic inflammatory response syndrome (NegIAI/TB/SIRS), or healthy mothers that delivered at term (NegIAI/TB). Differences between groups were analyzed by 1-way factorial ANCOVA after adjusting for gestational age at amniocentesis. IAI, intraamniotic infection or inflammation; PTB, preterm birth; SIRS, systemic inflammatory response syndrome; TB, term birth; AF, amniotic fluid; GA, gestational age; TSAT, transferrin saturation. The values in the table are means adjusted for gestational age at amniocentesis. [A]$P < 0.05$; [B]$P < 0.01$; [C]$P < 0.001$. *P* value by ANCOVA compared with PosIAI/PTB.

maternal inflammation, hepcidin, and hypoferremia, raising the question of the relative contribution of fetal versus maternal inflammation to the regulation of fetal serum iron. In our rhesus macaque model of LPS- or *Ureaplasma*-induced IAI, only fetuses, but not dams, had detectable inflammation. Nevertheless, rhesus macaque fetal hepcidin was increased and fetal plasma iron was decreased, confirming the role of fetal, rather than maternal hepcidin, in regulating fetal plasma iron levels. In both mouse and rhesus macaque models, despite detectable increases in amniotic fluid hepcidin, amniotic fluid iron was relatively low and stable, presumably because fetal iron is not exported into the fluid by the organs that contribute to amniotic fluid formation. Iron may even be absorbed from the amniotic fluid by iron transporters in the fetal intestine and possibly lung, which may be advantageous during rapid fetal growth. Hepcidin accumulation in amniotic fluid is likely a result of filtration or excretion of fetal plasma hepcidin by the kidneys. Indeed, we observed a strong correlation between fetal hepcidin and matching amniotic fluid hepcidin in mice and macaques.

Recently described as "intrauterine inflammation or infection or both (Triple I)," chorioamnionitis is a common cause of preterm birth and adverse neonatal and perinatal outcomes in humans (37, 38). In humans, *Ureaplasma* is commonly isolated bacteria from amniotic fluid in the setting of preterm birth with or without clinical chorioamnionitis (39–41), yet a significant percentage of cases with intraamniotic detection of *Ureaplasma* show no histological inflammation (42). In our macaque model, we did not observe any induction in inflammatory cytokines or hepcidin in maternal plasma, cord blood plasma, or amniotic fluid when measured 3 days after intraamniotic inoculation, indicating the absence of strong inflammation in that model. However, using LPS as a stronger inflammatory stimulus, our mouse and rhesus macaque models show that both systemic inflammation and IAI stimulate hepcidin production in the fetus, which in turn lowers iron levels in fetal blood but not amniotic fluid. Although our animal models were treated with exogenous LPS, we observed a similar fetal response to IAI in human pregnancy. Human fetuses exposed antenatally to IAI had elevated cord blood plasma hepcidin levels and consequently lower plasma iron concentrations and TSAT. Amniotic fluid from human fetuses exposed to IAI showed no changes in iron concentrations, despite higher levels of amniotic fluid hepcidin. The ability of the fetus to respond to inflammatory signals by decreasing iron concentration in fetal circulation and sequestering iron away from bacteria may be an important protective mechanism during intraamniotic infections. However, with chronic inflammation, prolonged fetal hepcidin induction and hypoferremia could become detrimental by causing iron restriction in the fetus, leading to decreased iron availability to fetal tissues and possibly anemia.

Our data indicate that iron concentrations in amniotic fluid are much lower than in fetal or maternal circulation in all species examined (mice, macaques, and humans). Interestingly, although TSAT was high in mouse amniotic fluid, it was low in human amniotic fluid from the end of second and third trimester. Thus, although unregulated, low TSAT in humans indicates a low risk of NTBI generation in amniotic fluid, and this may be an important protective factor during intraamniotic infections. The rapid induction of

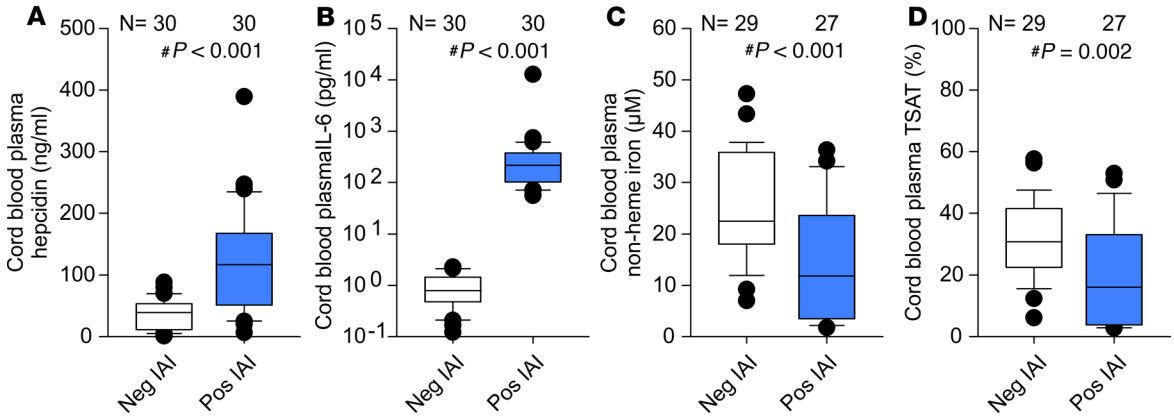

Figure 6. Cord blood iron homeostasis in healthy and complicated human pregnancy. Cord blood from the umbilical vein was sampled at the time of delivery from singleton preterm human fetuses (<34 weeks of gestational age) with or without antenatal exposure to intraamniotic infection. Measurements at time of delivery in cord blood plasma: (**A**) hepcidin, (**B**) IL-6, (**C**) non-heme iron, and (**D**) transferrin saturation. Statistical differences between groups were determined by 1-way ANOVA on ranks followed by Dunn's method for multiple comparisons (as indicated by #). The number of samples are reported above the box plot for each figure panel.

fetal hepcidin by inflammation and consequent hypoferremia in all 3 species (mice, rhesus macaques, and humans) demonstrates a conserved mechanism that may be important in fetal host defense.

Methods

Mouse experiments. WT C57BL/6J mice were obtained from The Jackson Laboratory or bred in the UCLA vivarium. Hepcidin-1–knockout (*Hamp*$^{-/-}$) mice were originally provided to our laboratory by Sophie Vaulont (Institut Cochin, Université Paris Descartes, Paris, France) (43) and were backcrossed to C57BL/6J mice. Mice were housed in a barrier facility under standard laboratory conditions. Unless otherwise specified, mice were maintained on a laboratory chow diet containing 185 ppm iron as ferrous carbonate (Rodent Diet 20 5053, PicoLab). This group was referred to as "iron-replete" (having normal iron stores).

To model iron deficiency during pregnancy, WT mice were fed a purified low-iron diet containing 4 ppm carbonyl iron (TD.80396, Envigo-Teklad) starting at E10.5 and for the duration of pregnancy. To assess the condition of iron overload, we used *Hamp*$^{-/-}$ mice, which become naturally iron loaded when fed standard chow. Iron-deficient and iron-loaded dams were compared with iron-replete WT controls fed standard chow. For these studies, samples were harvested at E18.5. Complete blood counts in maternal blood were performed using a Hemavet 950FS automated analyzer (Drew Scientific). Three to five fetuses from each litter were selected for analysis.

To induce maternal systemic inflammation, pregnant iron-replete WT mice at E15.5 (80% of term gestation) were weighed and injected subcutaneously in the interscapular area with a single dose of 0.5 μg/g LPS (*E. coli* serotype O55:B5, MilliporeSigma) or sterile water. At the indicated times, mice were euthanized by isoflurane overdose and tissues were collected for analysis. For these studies, fetal serum from the entire litter was pooled to generate sufficient volume for analysis.

Mouse amniotic fluid was collected by syringe from individual gestational sacs (50–100 μL per fetus) either at E16.5 (inflammation studies) or E18.5 (iron studies).

Terminology. In literature related to mouse pregnancy studies, the term "embryo" is used to define all stages of murine development in utero. However, because we studied 3 different species in this manuscript, for simplicity we used the term "fetus" for all the species, including the mouse.

Nonhuman primate studies. Adult female rhesus macaques (*Macaca mulatta*) were maintained at the California National Primate Research Center at the University of California, Davis (UCD). To induce IAI, time-mated pregnant rhesus macaques at 130 days gestation (80% of term pregnancy) received by ultrasound-guided intraamniotic injection either 1 mL saline for 16 hours (n = 5), 1 mg LPS (MilliporeSigma Sigma) in 1 mL saline solution (n = 5) for 16 hours, or *Ureaplasma parvum* serovar 1 (1×10^7 CFU) (n = 5) for 3 days. Some animals had maternal blood and amniotic fluid drawn before injections, and those samples were included in the control group. At the indicated times, pregnant dams were surgically delivered, and samples were collected for analysis. Infection and inflammation were confirmed histologically by the

presence of neutrophil infiltration. There were no spontaneous deaths or preterm labor in all groups. Some of the animals used in this study were previously reported (30, 44).

Human samples. We studied 124 human amniotic fluid samples from women that were tested because of clinical suspicion of IAI, independent of the research protocol. Clinical suspicion of IAI included preterm labor with contractions persistent despite tocolysis, advanced cervical dilation, and/or preterm prelabor rupture of the membranes. Gestational age at amniotic fluid sampling as well as gestational age at delivery are shown in Table 2. In all cohorts, amniotic fluid was collected by ultrasound-guided amniocentesis. Amniotic fluid was cultured for aerobic and anaerobic bacteria, *Ureaplasma urealyticum* and *Mycoplasma hominis*. IAI was defined by positive culture or positive Gram stain. Additional clinical laboratory tests were performed to confirm or rule-out IAI. Cord blood was not available for analysis. Preterm labor was defined as the presence of regular uterine contractions and documented cervical effacement and/or dilation in patients under 37 weeks of gestation.

The amniotic fluid samples were analyzed in 4 groups: PosIAI/PTB (n = 72), NegIAI/PTB (n = 22), NegIAI/TB (n = 20), and NegIAI/TB/SIRS (n = 10).

In a separate human cohort with available cord blood but not amniotic fluid, we evaluated 60 human cord blood samples from singleton preterm infants with or without antenatal exposure to IAI. Cord blood was obtained by aseptic puncture of the clamped umbilical vein at the time of delivery (30.6 ± 2.8 weeks of gestation, range: 24.1–33.6). The fetal exposure to IAI was defined by IL-6 as previously described (38, 45, 46).

Non-heme iron measurement. Maternal liver iron was measured as previously described (Iron-SL 157-30, Sekisui Diagnostics) (8). Serum was obtained from maternal and fetal mouse blood by centrifugation at 2,700 *g* for 10 minutes. Serum iron concentration was measured by colorimetric spectrophotometry using an iron calibrator. Serum iron in mouse samples and plasma iron in human samples was measured using the Sekisui Diagnostics Iron-SL kit (catalog 157-30): 260 μL R1 reagent was added to 20 μL standard, blank, or sample. Absorbance at 595 nm (A1) was measured before adding 60 μL R2 for 5 minutes, after which absorbance at 595 nm was remeasured (A2). Plasma iron in rhesus macaque samples was measured using the Genzyme iron total kit (catalog 102-25): 150 μL R1 reagent was added to 20 μL standard (DC-Cal Se-035, Sekisui), blank, or sample. Absorbance at 560 nm (A1) was measured before adding 50 μL R2 and remeasured at 560 nm (A2) after addition of R2. Plasma, serum, or amniotic fluid iron were calculated in μM as = (Δsample A2 – A1/Δstandard A2 – A1) × standard concentration.

TF and TSAT measurement. TF concentrations in human and mouse samples were determined by ELISA according to the manufacturer's instructions (TF ELISA kit, Alpha Diagnostics, 1210 human, 6390 mouse). TF concentrations measured in ng/mL were converted to μM using the molecular weight of TF (~80 kDa), and total iron binding capacity (TIBC) was calculated by multiplying TF in μM by 2 to account for the 2 iron binding sites. TIBC was used in combination with serum iron measurements to calculate TSAT. TSAT (%TSAT) = (serum iron/TIBC) × 100. This method could not accurately and reproducibly determine TF concentrations in rhesus macaque samples.

Hepcidin assays. For human and rhesus macaque samples, hepcidin protein concentrations in plasma and amniotic fluid were measured by ELISA according to the manufacturer's instructions (rhesus macaque, Intrinsic Hepcidin IDx; Human amniotic fluid, DRG Diagnostics; human cord blood, Intrinsic Hepcidin IDx). Hepcidin protein concentration in mouse serum and amniotic fluid was determined by ELISA using Ab2B10 (capture) and Ab2H4-HRP (detection) antibodies provided by Amgen, and synthetic mouse hepcidin-25 was used to generate standard curves ranging from 400 to 3.2 pg/mL (47).

Inflammation assays. In mouse studies, presence of inflammation was assessed by mRNA expression of serum amyloid A-1 (*Saa-1*) (48) and hepcidin (*Hamp*) in maternal liver. In macaque studies, concentrations of cytokines TNF-α, MCP-1, IL-1β, and IL-6 in amniotic fluid, maternal plasma, and cord blood plasma were determined by Luminex using non-human primate multiplex kits (MilliporeSigma). In human samples, concentrations of IL-6 in amniotic fluid and cord blood plasma samples were measured by ELISA (Pierce-Endogen).

Gene expression quantification by qRT-PCR. Frozen mouse liver pieces were homogenized in TRIzol Reagent (Life Technologies). Total RNA was isolated by chloroform extraction, and 1 μg RNA was reverse transcribed using the iScript cDNA Synthesis Kit (Bio-Rad). Quantitative real-time PCR was performed on cDNA using SsoAdvanced SYBER Green Supermix (Bio-Rad) on the CFX Real-Time PCR Detection System (Bio-Rad). Samples were measured in duplicate and normalized to *Hprt* or *Rpl4* using the following primer sequences: *Hprt* forward 5′-CTGGTTAAGCAGTACAGCCCCAA-3′ and reverse 5′-CAGGAGGTCCTTTTCACCAGC-3′, *Rpl4* forward 5′-TGAAAAGCCCAGAAATCCAA-3′ and reverse

5′-AGTCTTGGCGTAAGGGTTCA-3′; *Saa1* forward 5;-AGTCTGGGCTGCTGAGAAAA-3′ and reverse 5′-ATGTCTGTTGGCTTCCTGGT-3′, *Hamp1* forward 5′-AAGCAGGGCAGACATTGCGAT-3′ and reverse 5′-CAGGATGTGGCTCTAGGCTATGT-3′. Data are expressed as $2^{-\Delta\Delta Ct\ (housekeeping\text{-}target)}$.

Statistics. All data are presented as box-and-whisker plots. The box portion indicates the upper 75th and lower 25th percentile, whiskers indicate variability outside the upper 90th and lower tenth percentile, and individual points represent outliers. The solid line within the box indicates the median. Statistical analysis was performed using SigmaPlot version 12.5 (Systat Software). Statistical differences between groups were determined by 1-way ANOVA followed by Holm-Sidak for multiple comparisons for normally distributed values, 1-way ANOVA on ranks followed by Dunn's method for multiple comparisons of nonparametric values, 2-tailed Student's *t* test for normally distributed values, or Mann-Whitney *U* test for nonparametric values. Adjustment for gestational age and comparison of groups in human amniotic fluid samples was done using factorial and 1-way ANOVA (VassarStats). The number of animals in each group is indicated in the graphs. *P* values of less than 0.05 were considered significant.

Study approval. All animal studies were approved by the Institutional Animal Care and Use Committees at UCLA (for mouse studies) and UCD (for macaque studies) and were carried out in accordance with the *Guide for the Care and Use of Laboratory Animals* (National Academies Press, 2011). Human studies were approved by the Institutional Review Boards at Yale University and The Ohio State University, where the samples were collected, and all women signed informed consent.

Author contributions

ALF designed and performed experiments, analyzed data, and wrote the manuscript. VS and PP performed experiments and assisted with data interpretation. SGK, CAC, and AHJ provided rhesus macaque samples and assisted with data interpretation. ST measured amniotic fluid hepcidin concentration in human amniotic fluid samples, collected cord blood samples from the first cohort, and assisted with data interpretation. CSB enrolled human subjects, collected specimens, abstracted human data, and assisted with data interpretation. IAB provided human samples and assisted with data interpretation. TG and EN conceived the project, analyzed data, and wrote the manuscript. All authors contributed edits to the manuscript and approved the final version.

Acknowledgments

This study was supported by National Center for Advancing Translational Sciences UCLA Clinical and Translational Science Institute grants UL1TR000124, UL1TR001881, and R01 HD096863 (to EN), NIH Ruth L. Kirschstein National Research Service Awards T32GM065823 and F31HD097931 (to AF), NIH grants R21HD90856 and R01HD 98389 (to SGK), NIH grant U01 ES029234, a Burroughs Wellcome grant, and Cincinnati Children's Hospital Medical Center Perinatal Infection and Inflammation Collaborative (to CAC).

Address correspondence to: Elizabeta Nemeth, 10833 LeConte Ave., CHS 43-229, Los Angeles, California 90095, USA. Phone: 310.825.2841; Email: enemeth@mednet.ucla.edu.

1. Breuer W, Ronson A, Slotki IN, Abramov A, Hershko C, Cabantchik ZI. The assessment of serum nontransferrin-bound iron in chelation therapy and iron supplementation. *Blood*. 2000;95(9):2975–2982.
2. Evans P, Cindrova-Davies T, Muttukrishna S, Burton GJ, Porter J, Jauniaux E. Hepcidin and iron species distribution inside the first-trimester human gestational sac. *Mol Hum Reprod*. 2011;17(4):227–232.
3. Gazzolo D, et al. Non protein bound iron concentrations in amniotic fluid. *Clin Biochem*. 2005;38(7):674–677.
4. Hattori Y, et al. Catalytic ferrous iron in amniotic fluid as a predictive marker of human maternal-fetal disorders. *J Clin Biochem Nutr*. 2015;56(1):57–63.
5. Legge M. Second trimester amniotic fluid ferritin and transferrin levels in normal and anencephalic pregnancies. *J Obstet Gynaecol (Lahore)*. 1983;4(1):14–15.
6. Larsen B, Snyder IS, Galask RP. Transferrin concentration in human amniotic fluid. *Am J Obstet Gynecol*. 1973;117(7):952–954.
7. Emerit J, Beaumont C, Trivin F. Iron metabolism, free radicals, and oxidative injury. *Biomed Pharmacother*. 2001;55(6):333–339.
8. Stefanova D, et al. Endogenous hepcidin and its agonist mediate resistance to selected infections by clearing non-transferrin-bound iron. *Blood*. 2017;130(3):245–257.
9. Park CH, Valore EV, Waring AJ, Ganz T. Hepcidin, a urinary antimicrobial peptide synthesized in the liver. *J Biol Chem*. 2001;276(11):7806–7810.
10. Nemeth E, et al. Hepcidin regulates cellular iron efflux by binding to ferroportin and inducing its internalization. *Science*. 2004;306(5704):2090–2093.
11. Aschemeyer S, et al. Structure-function analysis of ferroportin defines the binding site and an alternative mechanism of action of hepcidin. *Blood*. 2018;131(8):899–910.

12. Ganz T. Hepcidin and iron regulation, 10 years later. *Blood*. 2011;117(17):4425–4433.
13. Nemeth E, et al. IL-6 mediates hypoferremia of inflammation by inducing the synthesis of the iron regulatory hormone hepcidin. *J Clin Invest*. 2004;113(9):1271–1276.
14. Nicolas G, et al. The gene encoding the iron regulatory peptide hepcidin is regulated by anemia, hypoxia, and inflammation. *J Clin Invest*. 2002;110(7):1037–1044.
15. Nemeth E, Valore EV, Territo M, Schiller G, Lichtenstein A, Ganz T. Hepcidin, a putative mediator of anemia of inflammation, is a type II acute-phase protein. *Blood*. 2003;101(7):2461–2463.
16. Pigeon C, et al. A new mouse liver-specific gene, encoding a protein homologous to human antimicrobial peptide hepcidin, is overexpressed during iron overload. *J Biol Chem*. 2001;276(11):7811–7819.
17. Bothwell TH. Iron requirements in pregnancy and strategies to meet them. *Am J Clin Nutr*. 2000;72(1 Suppl):257S–264S.
18. Fisher AL, Nemeth E. Iron homeostasis during pregnancy. *Am J Clin Nutr*. 2017;106(Suppl 6):1567S–1574S.
19. Bah A, et al. Serum hepcidin concentrations decline during pregnancy and may identify iron deficiency: analysis of a longitudinal pregnancy cohort in The Gambia. *J Nutr*. 2017;147(6):1131–1137.
20. van Santen S, Kroot JJ, Zijderveld G, Wiegerinck ET, Spaanderman ME, Swinkels DW. The iron regulatory hormone hepcidin is decreased in pregnancy: a prospective longitudinal study. *Clin Chem Lab Med*. 2013;51(7):1395–1401.
21. Rehu M, et al. Maternal serum hepcidin is low at term and independent of cord blood iron status. *Eur J Haematol*. 2010;85(4):345–352.
22. Sangkhae V, et al. Effects of maternal iron status on placental and fetal iron homeostasis. *J Clin Invest*. 2020;130(2):625–640.
23. Young MF, et al. Maternal hepcidin is associated with placental transfer of iron derived from dietary heme and nonheme sources. *J Nutr*. 2012;142(1):33–39.
24. Bastin J, Drakesmith H, Rees M, Sargent I, Townsend A. Localisation of proteins of iron metabolism in the human placenta and liver. *Br J Haematol*. 2006;134(5):532–543.
25. Sangkhae V, Nemeth E. Placental iron transport: The mechanism and regulatory circuits. *Free Radic Biol Med*. 2019;133:254–261.
26. Nicolas G, et al. Severe iron deficiency anemia in transgenic mice expressing liver hepcidin. *Proc Natl Acad Sci USA*. 2002;99(7):4596–4601.
27. Willemetz A, et al. Matriptase-2 is essential for hepcidin repression during fetal life and postnatal development in mice to maintain iron homeostasis. *Blood*. 2014;124(3):441–444.
28. Tabbah SM, et al. Hepcidin, an iron regulatory hormone of innate immunity, is differentially expressed in premature fetuses with early-onset neonatal sepsis. *Am J Perinatol*. 2018;35(9):865–872.
29. Presicce P, et al. Neutrophil recruitment and activation in decidua with intra-amniotic IL-1beta in the preterm rhesus macaque. *Biol Reprod*. 2015;92(2):56.
30. Presicce P, et al. IL-1 signaling mediates intrauterine inflammation and chorio-decidua neutrophil recruitment and activation. *JCI Insight*. 2018;3(6):98306.
31. Silberstein T, Saphier M, Mashiach Y, Paz-Tal O, Saphier O. Elements in maternal blood and amniotic fluid determined by ICP-MS. *J Matern Fetal Neonatal Med*. 2015;28(1):88–92.
32. Tamura T, et al. Relationship between amniotic fluid and maternal blood nutrient levels. *J Perinat Med*. 1994;22(3):227–234.
33. Kocyłowski R, et al. Evaluation of essential and toxic elements in amniotic fluid and maternal serum at birth. *Biol Trace Elem Res*. 2019;189(1):45–54.
34. Thadepalli H, Gangopadhyay PK, Maidman JE. Amniotic fluid analysis for antimicrobial factors. *Int J Gynaecol Obstet*. 1982;20(1):65–72.
35. Oka K, Hagio Y, Tetsuoh M, Kawano K, Hamada T, Kato T. The effect of transferrin and lysozyme on antibacterial activity of amniotic fluid. *Biol Res Pregnancy Perinatol*. 1987;8(1 1ST Half):1–6.
36. Evans HE, Levy E, Glass L. Effect of amniotic fluid on bacterial growth. *Obstet Gynecol*. 1977;49(1):35–37.
37. Peng CC, Chang JH, Lin HY, Cheng PJ, Su BH. Intrauterine inflammation, infection, or both (Triple I): A new concept for chorioamnionitis. *Pediatr Neonatol*. 2018;59(3):231–237.
38. Tita AT, Andrews WW. Diagnosis and management of clinical chorioamnionitis. *Clin Perinatol*. 2010;37(2):339–354.
39. Cassell GH, Waites KB, Watson HL, Crouse DT, Harasawa R. Ureaplasma urealyticum intrauterine infection: role in prematurity and disease in newborns. *Clin Microbiol Rev*. 1993;6(1):69–87.
40. Kasper DC, et al. The bacterial load of Ureaplasma parvum in amniotic fluid is correlated with an increased intrauterine inflammatory response. *Diagn Microbiol Infect Dis*. 2010;67(2):117–121.
41. Cox C, et al. The common vaginal commensal bacterium Ureaplasma parvum is associated with chorioamnionitis in extreme preterm labor. *J Matern Fetal Neonatal Med*. 2016;29(22):3646–3651.
42. Revello R, et al. Prediction of chorioamnionitis in cases of intraamniotic infection by ureaplasma urealyticum in women with very preterm premature rupture of membranes or preterm labour. *J Matern Fetal Neonatal Med*. 2018;31(14):1839–1844.
43. Lesbordes-Brion JC, et al. Targeted disruption of the hepcidin 1 gene results in severe hemochromatosis. *Blood*. 2006;108(4):1402–1405.
44. Senthamaraikannan P, et al. Intra-amniotic Ureaplasma parvum-induced maternal and fetal inflammation and immune responses in rhesus macaques. *J Infect Dis*. 2016;214(10):1597–1604.
45. Romero R, Yoon BH, Kenney JS, Gomez R, Allison AC, Sehgal PB. Amniotic fluid interleukin-6 determinations are of diagnostic and prognostic value in preterm labor. *Am J Reprod Immunol*. 1993;30(2-3):167–183.
46. Romero R, et al. A comparative study of the diagnostic performance of amniotic fluid glucose, white blood cell count, interleukin-6, and gram stain in the detection of microbial invasion in patients with preterm premature rupture of membranes. *Am J Obstet Gynecol*. 1993;169(4):839–851.
47. Kim A, et al. A mouse model of anemia of inflammation: complex pathogenesis with partial dependence on hepcidin. *Blood*. 2014;123(8):1129–1136.
48. Gabay C, Kushner I. Acute-phase proteins and other systemic responses to inflammation. *N Engl J Med*. 1999;340(6):448–454.